



**HAL**  
open science

## Data driven design of tonal noise feedback cancellers

Raúl Antonio Meléndez, Ioan Doré Landau, Luc Dugard, Gabriel Buche

► **To cite this version:**

Raúl Antonio Meléndez, Ioan Doré Landau, Luc Dugard, Gabriel Buche. Data driven design of tonal noise feedback cancellers. IFAC WC 2017 - 20th IFAC World Congress, Jul 2017, Toulouse, France. pp. 916 - 921. hal-01394269

**HAL Id: hal-01394269**

**<https://hal.science/hal-01394269>**

Submitted on 9 Nov 2016

**HAL** is a multi-disciplinary open access archive for the deposit and dissemination of scientific research documents, whether they are published or not. The documents may come from teaching and research institutions in France or abroad, or from public or private research centers.

L'archive ouverte pluridisciplinaire **HAL**, est destinée au dépôt et à la diffusion de documents scientifiques de niveau recherche, publiés ou non, émanant des établissements d'enseignement et de recherche français ou étrangers, des laboratoires publics ou privés.

# Data driven design of tonal noise feedback cancellers

Raúl A. Meléndez <sup>\*,\*</sup>, Ioan D. Landau <sup>\*</sup>, Luc Dugard <sup>\*</sup>, Gabriel Buche <sup>\*</sup>

<sup>\*</sup> Univ. Grenoble Alpes, CNRS, GIPSA-lab, F-38000 Grenoble, France,  
(e-mail: Raul.Melendez, Ioan-Dore.Landau, Luc.Dugard,  
Gabriel.Buche@gipsa-lab.grenoble-inp.fr)

---

**Abstract:** This paper emphasizes the design methodology for active tonal noise feedback cancellers starting from data collected on the system. To design such control systems, an accurate dynamic model of the system is necessary. Physical modeling can provide qualitative results but fails to yield enough accurate models for control design. The main point in the methodology is identification of primary path (noise propagation) and secondary path (compensation) models from data. The procedure is investigated in details starting with transfer functions' order estimations, continuing with parameters estimation and model's validation. The second aspect is the design of a noise canceller using the Internal Model Principle and the sensitivity function shaping in order to reduce the "water-bed" effect. The estimated model's quality for control design is illustrated by the experimental performance of a tonal noise feedback canceller implemented on a test bench.

*Keywords:* Active noise control, System Identification, Internal model principle, Band stop filters, Sensitivity functions.

---

## 1. INTRODUCTION

Active noise control (ANC) has been under research for many years and applied in various kind of applications. In most cases feed-forward broadband noise compensation is currently used for ANC when a disturbance's image is available (correlated measurement with the disturbance). See Elliott and Nelson (1994), Elliott and Sutton (1996), Kuo and Morgan (1999), Zeng and de Callafon (2006).

However, these solutions, inspired by Widrows technique for adaptive noise cancellation, see Widrow and Stearns (1985), ignore the possibilities offered by feedback control systems and have a number of disadvantages: they require the use of an additional transducer, difficult choice for its location and presence, in most cases, of a "positive" coupling between the compensator system and the disturbance image's measurement, which can cause instabilities. To achieve the disturbance's rejection (asymptotically) without measuring it, a feedback solution can be considered.

Residual noise can be described as the result of acoustic waves which pass through the system, and the noise cancellers' objective is to attenuate it. In many cases, these waves can be characterized in the frequency domain either as tonal disturbances or as narrow band perturbations. The common framework is the assumption that a narrow band disturbance is the result of a white noise or a Dirac impulse passed through the "disturbance's model." In the case of tonal (narrow band) noise disturbances, the basic idea is to use the "internal model principle" to get a strong attenuation, combined with output sensitivity function shaping, in order to avoid unwanted amplifications in the tonal disturbances' neighborhoods.

However, the real time performance of the noise cancellers strongly depends on the secondary path dynamic model's quality used for designing the feedback control law. Many studies have been carried out to develop dynamic models for control design, starting from the basic physical equations describing the system and trying to determine, from the systems' geometry, the values of some basic constants. See Nelson and Elliott (1993). Zimmer and Lipshitz (2003) give a very complete evaluation of the physical modeling in the context of active noise control in ducts. Unfortunately on one hand the resulting models are not very good, since it is hard for a given system to find the correct physical constants, and on the other hand it is a PDE model for which there are not simple control design methods available.

What is needed in practice is a finite dimension discrete-time model which reproduces the system's dynamical behavior. Once such a model is available, one can use digital control design techniques readily implementable on a real time computer. These models can be obtained directly from data using system identification techniques, see Ljung (1999); Landau et al. (2016); Carmona and Alvarado (2000). However these discrete-time models for active noise compensation present a number of peculiarities which require to develop a specific identification procedure. One of the major objectives of the paper is to clarify how system identification from data should be done in the context of active noise control. Previous identification results given in Ben Amara et al. (1999) and Zeng and de Callafon (2006) have been also considered.

The final quality test for an identified model is to verify how close are the real-time experimental results obtained and the designed controller's performances in simulation. As shown later, the results are very close, which indicates that the proposed procedure is reliable. Two control problems have been considered: the rejection of two tonal disturbances, and strong

---

<sup>\*</sup> Financial support thanks to Consejo Nacional de Ciencia y Tecnología de México, CONACyT.

attenuation of interferences, caused by tonal disturbances with very close frequencies. The Internal Model Principle (*IMP*) combined with the sensitivity functions' shaping will be used for control design.

## 2. EXPERIMENTAL SETUP

The test bench used for the experiments is shown in Fig. 1, and its detailed scheme is given in Fig. 2. The speaker used as the source of disturbances is labeled as 1, the control speaker is 2 and finally, at pipe's open end, the microphone that measures the system's output (residual noise) is denoted as 3. The transfer function between the disturbance's speaker and the microphone (1→3) is denominated *Primary Path*, while the transfer function between the control speaker and the microphone (2→3) is denominated *Secondary Path*. Both speakers are connected to a xPC Target computer with Simulink Real Time<sup>®</sup> environment through a pair of high definition power amplifiers and a data acquisition card. The current signals  $u(t)$  and  $p(t)$  are amplified and reach the speakers' voice coils and displace them, generating movement in the diaphragms and thus, sound waves. In Fig. 2,  $y(t)$  is the system's output (residual noise measurement). Both primary and secondary paths have a double differentiator behavior, since as input we have the voice coil displacement, and as output the air acoustic pressure. A second computer is used for development, design and operation with Matlab<sup>®</sup>.

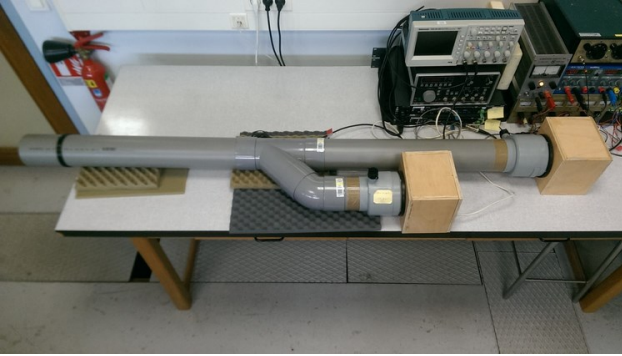


Fig. 1: Noise control test bench (Photo).

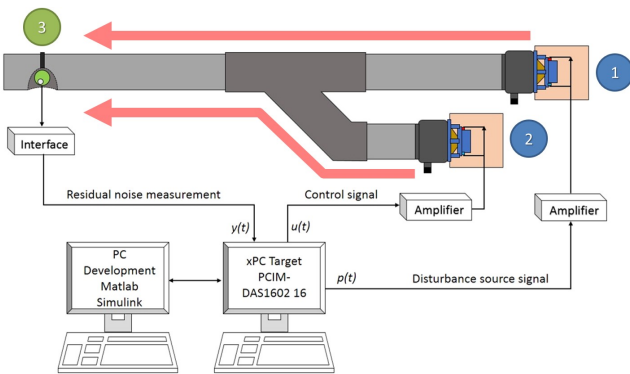


Fig. 2: Noise control test bench diagram.

PVC pipes of 0.10 m diameter are used in this test bench, with couplings of 135° for the control speaker. Distances between disturbance speaker and microphone are 1.65 m, and to control input 0.80 m. Speakers are isolated inside wood boxes filled with special foam in order to create anechoic chambers and reduce the radiation noise produced.

## 3. SYSTEM DESCRIPTION

The linear time invariant (*LTI*) discrete-time model of the secondary path, or plant, used for controller design is

$$G(z^{-1}) = \frac{z^{-d}B(z^{-1})}{A(z^{-1})} = \frac{z^{-d}B'(z^{-1})}{A(z^{-1})}D_F(z^{-1}), \quad (1)$$

where  $D_F(z^{-1})$  is a double differentiator filter and

$$A(z^{-1}) = 1 + a_1z^{-1} + \dots + a_{n_A}z^{-n_A}, \quad (2)$$

$$B'(z^{-1}) = b_1z^{-1} + \dots + b_{n_{B'}}z^{-n_{B'}}, \quad (3)$$

with  $d$  as the plant pure time delay in number of sampling periods<sup>1</sup>. The system's order is

$$n = \max(n_A, n_{B'} + d) \quad (4)$$

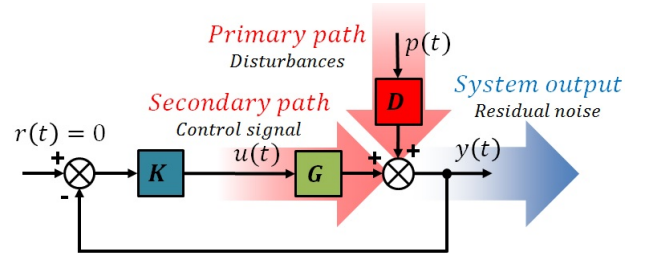


Fig. 3: Feedback regulation scheme.

Figure 3 shows the closed loop feedback regulation scheme, where the controller  $K$  is described by

$$K(z^{-1}) = \frac{R}{S} = \frac{r_0 + r_1z^{-1} + \dots + r_{n_R}z^{-n_R}}{1 + s_1z^{-1} + \dots + s_{n_S}z^{-n_S}}. \quad (5)$$

The plant's output  $y(t)$  and the input  $u(t)$  may be written as (see Fig. 3):

$$y(t) = \frac{q^{-d}B(q^{-1})}{A(q^{-1})} \cdot u(t) + p(t), \quad (6)$$

$$S(q^{-1}) \cdot u(t) = -R(q^{-1}) \cdot y(t). \quad (7)$$

In (6),  $p(t)$  is the disturbances' effect on the measured output<sup>2</sup> and  $R(z^{-1})$ ,  $S(z^{-1})$  are polynomials in  $z^{-1}$  having the following expressions:

$$R = H_R \cdot R' = H_R \cdot (r'_0 + r'_1z^{-1} + \dots + r'_{n_{R'}}z^{-n_{R'}}), \quad (8)$$

$$S = H_S \cdot S' = H_S \cdot (1 + s'_1z^{-1} + \dots + s'_{n_{S'}}z^{-n_{S'}}), \quad (9)$$

where  $H_S(z^{-1})$  and  $H_R(z^{-1})$  represent prespecified parts of the controller (used for example to incorporate the internal model of a disturbance, or to open the loop at some frequencies) and  $S'(z^{-1})$  and  $R'(z^{-1})$  are solutions of the Bezout equation:

$$P = (A \cdot H_S) \cdot S' + (z^{-d}B \cdot H_R) \cdot R'. \quad (10)$$

In (10)  $P(z^{-1})$  represents the characteristic polynomial, which specifies the desired closed loop poles of the system.

The transfer functions between the disturbance  $p(t)$  and the system's output  $y(t)$  and the control input  $u(t)$ , denoted respectively *output sensitivity* and *input sensitivity functions*, are given by

$$S_{yp}(z^{-1}) = \frac{A(z^{-1})S(z^{-1})}{P(z^{-1})} \quad (11)$$

<sup>1</sup> The complex variable  $z^{-1}$  is used to characterize the system's behavior in the frequency domain and the delay operator  $q^{-1}$  for the time domain analysis.

<sup>2</sup> The disturbance passes through the *primary path*, and  $p(t)$  is its output.

and

$$S_{up}(z^{-1}) = -\frac{A(z^{-1})R(z^{-1})}{P(z^{-1})}, \quad (12)$$

#### 4. DATA DRIVEN SYSTEM IDENTIFICATION

Model identification from experimental data is a well established methodology (see Landau et al. (2016); Ljung (1999)). Identification of systems is an experimental approach for determining a system's dynamic model. It includes four steps:

1. Input-output data acquisition under an experimental protocol and data pre-processing.
2. Estimation of the model complexity.
3. Estimation of the model parameters.
4. Validation of the identified model (complexity of the model and values of the parameters).

A complete identification operation must comprise the four stages indicated above. The typical input is a *PRBS*, which is a persistent excitation signal allowing unique parameter estimation even for high order system. Model validation is the final key point. It is important to emphasize that it does not exist one single algorithm that can provide in all the cases a good model (i.e. which passes the model validation tests). System identification should be viewed as an iterative process which has as objective to obtain a model which passes the model validation test and then can be used safely for control design. The procedure will be detailed for the secondary path's identification. The same methodology has been used for the primary path identification also (which is used only for simulation), and only the final results will be given.

##### 4.1 Data Acquisition under the experimental protocol

For design and application reasons (the objective is to reject tonal disturbances up to 400 Hz), the sampling frequency was selected as  $f_s = 2500$  Hz ( $T_s = 0.0004$ s) i.e. approximately 6 times the maximum frequency to attenuate, in accordance with recommendation given in (see Landau et al. (2016)). The theoretical band pass of the system is 1975 Hz, using formula given in Zimmer and Lipshitz (2003).

The experimental protocol should assure persistent excitation for the number of parameters to be estimated, thus a *PRBS* has been used. This signal's magnitude is constant allowing an easy selection with respect to the magnitude constraint on the plant input. One of the key points is the design of a *PRBS* in order to satisfy a compromise between the frequencies range to be covered (particularly those in the low frequencies region), and the test duration. One should apply at least on complete *PRBS* sequence, and its characteristics, including duration, will depend on the number of cells in the registers length used for its generation.

For identification, the signals' characteristics used in both paths are: magnitude = 0.15 V, register length = 17, frequency divider of 1, sequence length of  $2^{17} - 1 = 131,071$  samples, guaranteeing a uniform power spectrum from about 70 Hz to 1250 Hz. Since the transfer functions have a double differentiator behavior, this is considered as a system's known part and the objective will be to identify the unknown part only. To do this, the input sequence will be filtered by a double discrete-time differentiator  $D_F = (1 - q^{-1})^2$  such that  $u'(t) = D_F \cdot u(t)$ . The double differentiator will be concatenated with the identified model of the unknown part in the final models.

##### 4.2 Complexity Estimation

The basic idea in complexity estimation is to have, on one hand an unbiased estimator of the system parameters, which allows to obtain an unbiased evolution of the prediction error quadratic criterion that tends toward zero when the correct order is reached, and on the other hand a penalty term for the model's complexity. In order to get an unbiased estimation of the error criterion, the *instrumental variable* approach is used, see Landau et al. (2016); Duong and Landau (1996). As instrumental variables, delayed inputs are used,

$$Z(\hat{n}) = [U(t-L-1), U(t-1), U(t-L-2), U(t-2)\dots],$$

where  $L > n$  and

$$Y^T(t) = [y(t), y(t-1)\dots]; U^T(t) = [u'(t), u'(t-1)\dots].$$

Therefore the criterion used for the order estimation is:

$$V_{IV}(\hat{n}, N) = \min_{\hat{\theta}} \frac{1}{N} \|Y(t) - Z(\hat{n})\hat{\theta}\|^2, \quad (13)$$

where  $N$  is the number of samples. Adding a term which penalizes the model's complexity leads to

$$J_{IV}(\hat{n}, N) = V_{IV}(\hat{n}, N) + 2\hat{n} \frac{\log N}{N}, \quad (14)$$

with

$$\hat{n} = \min_{\hat{n}} J_{IV}. \quad (15)$$

When identifying finite dimensional discrete-time models,  $J_{IV}$  will show a minimum, function of  $n$ , allowing to define the estimated order of the model. Once an estimated order  $\hat{n}$  is selected, one can apply a similar procedure to estimate  $\hat{n}_A$ ,  $\hat{n} - \hat{d}$ , and  $\hat{n}_{B'} + \hat{d}$ , from which  $\hat{n}_A$ ,  $\hat{n}_{B'}$  and  $\hat{d}$  are obtained.

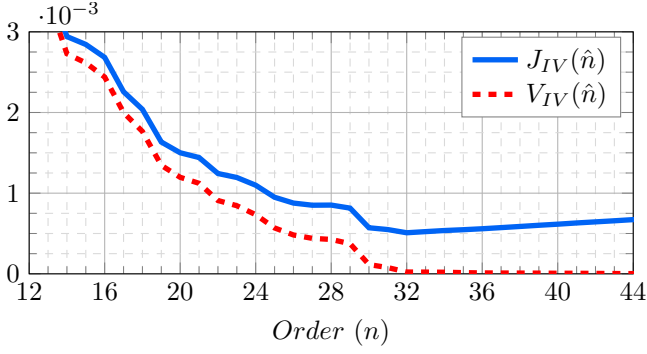
Results for the secondary path order estimation (without the double differentiator) are shown in Fig. 4 where both non-penalized and penalized criteria  $V_{IV}$ ,  $J_{IV}$  are represented. As it can be seen, the minimum is very flat (which is understandable since we are trying to approximate an infinite-dimensional system). It is therefore necessary to explore the model's properties for  $n$  between 36 and 41, in order to decide what order to take. Two additional criteria will be used to decide upon the best order estimation: I) comparison of the Power Spectral Density (*PSD*) of the identified model output, and that of the real data (in order to see if the identified model captures all the vibrations modes in the frequency range of operation) and II) comparison of the validation tests for the various models. To do this it is necessary to estimate the values of  $n_A$ ,  $n_{B'}$  and  $d$  for each order  $n$  selected, and to proceed with parameter estimation. To illustrate the details of orders estimations, the model with  $n = 40$  is considered. The procedure for other values of  $n$  is similar.

For the secondary path, Fig.4b shows that the minimum for  $n - d$  is 32. From Fig.4c one can see that the minimum for  $n_A$  is given by  $n_A = 38$ . From Fig.4d one concludes that  $n_{B'} + d = 38$ . Taking in account the definition of order  $n$ , one concludes that  $n_A = 38$ ,  $n_{B'} = 30$  and  $d = 8$ , therefore the effective estimated order of this model is  $n_e = 38$ . Similarly for the model with  $n = 38$ , one gets  $n_A = 37$ ,  $n_{B'} = 30$ ,  $d = 8$  (which means an effective order  $n_e = 38$ )<sup>3</sup>.

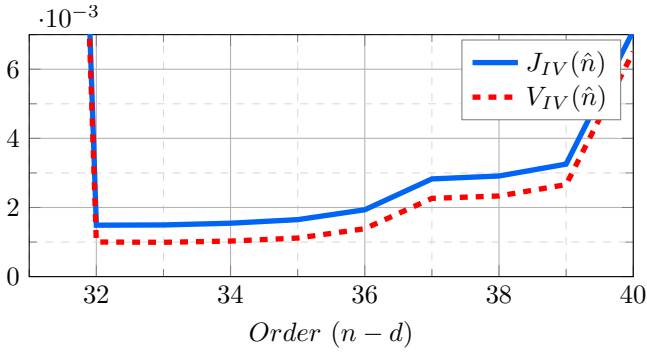
##### 4.3 Parameters Estimation

The algorithms used for parameter estimation will depend on the assumptions made on the measurements' noise characteristics, which have to be confirmed by the model validation.

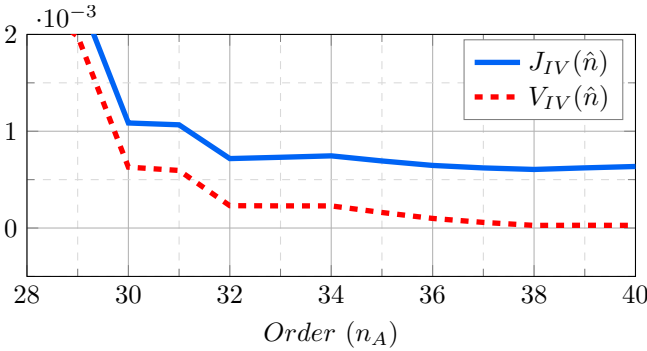
<sup>3</sup> Complete model's  $n_B = n_{B'} + 2$ , due to the double differentiator addition.



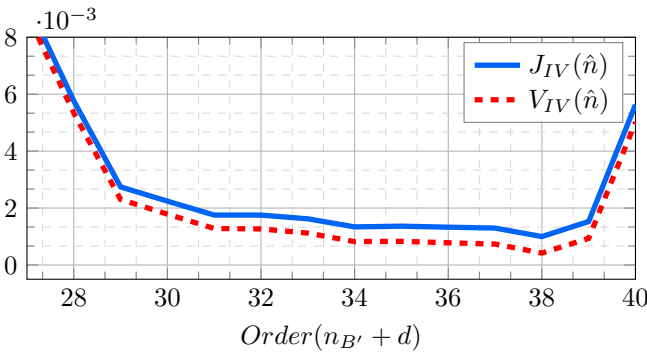
(a) Instrumental Variable ( $n$ ) order estimation.



(b) Instrumental Variable ( $n-d$ ) order estimation.



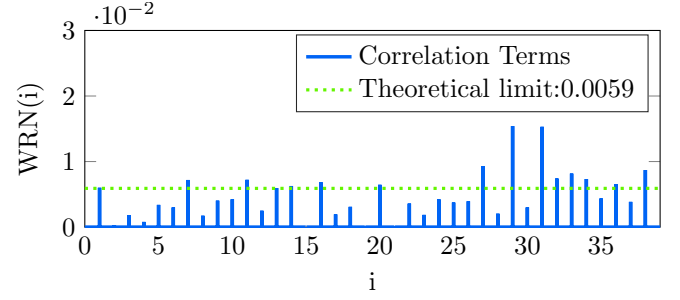
(c)  $n_A$  order estimation.



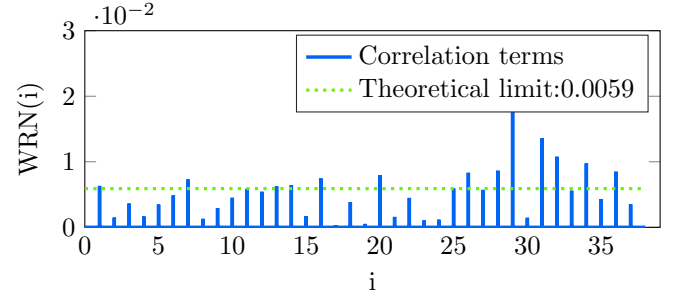
(d)  $n_{B'} + d$  order estimation.

Fig. 4: Secondary path, Instrumental Variable order estimation.

It is important to emphasize that no one single *plant + noise* structure exists that can describe all the situations encountered in practice. It is the validation stage which will allow to decide what method (and implicitly what noise model) has to be used.



(a) Model with  $n = 40$ .



(b) Model with  $n = 38$ .

Fig. 5: Whiteness validation tests for the secondary path.

Among the various identification methods used, it was found that Output Error with Extended Prediction Model (*XOLOE*) identification algorithm gives the best results in terms of validation for a given order model (see Landau et al. (2016)). It was concluded that the *ARMAX* model best represents the plant + noise model.

#### 4.4 Model Validation

The validation procedure associated with the identification of *ARMAX* models is based on a whiteness test.

*Whiteness test:* Let  $\{\varepsilon(t)\}$  be the centered (measured value minus average) sequence of the residual prediction errors. One computes estimations of the normalized autocorrelations as:

$$R(i) = \frac{1}{N} \sum_{t=1}^N \varepsilon(t)\varepsilon(t-i) \quad (16)$$

$$R(0) = \frac{1}{N} \sum_{t=1}^N \varepsilon^2(t); RN(i) = \frac{R(i)}{R(0)} \quad (17)$$

$$i = 1, 2, 3, \dots, n_A, \dots, n$$

One considers as a validation criterion (extensively tested on applications):

$$RN(0) = 1; |RN(i)| \leq \frac{2.17}{\sqrt{N}}; i \geq 1. \quad (18)$$

Fig. 5 shows the validation results (whiteness test) for the unknown part model with  $n = 40$  (effective  $n_e = 38$ ) and  $n = 38$  ( $n_e = 38$ ). The results are summarized in Table 1. Model  $n = 40$  leads to better results, which is confirmed in Fig. 6 where the PSD of real data's measures is compared with the two complete models outputs' PSD (including the double differentiator). Therefore the *XOLOE* model  $n = 40$  is chosen. It has 18 oscillatory modes with damping comprised between 0.0097 and 0.3129; also 13 pairs of oscillatory zeros

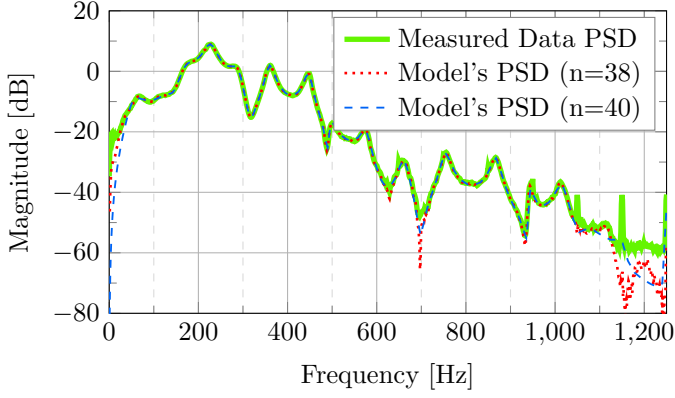


Fig. 6: System output PSD.

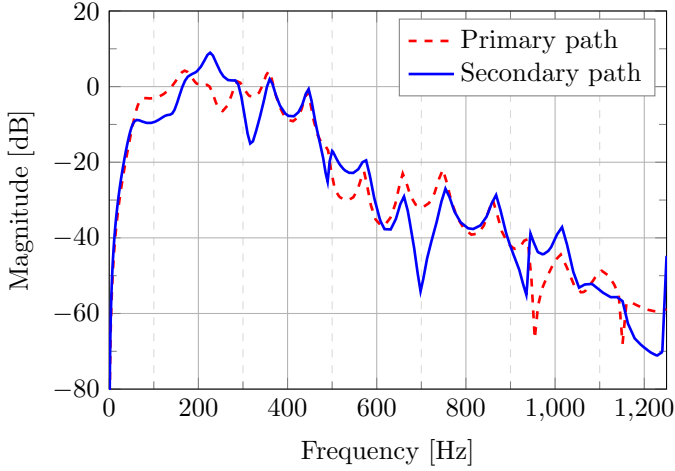


Fig. 7: Frequency characteristics of the identified primary and secondary paths models

with damping comprised between  $-0.0159$  and  $0.5438$ . The presence of these low damped zeros make the control system's design difficult. Fig. 7 gives the frequency characteristics of the identified complete models for the primary and secondary paths.

Table 1: Summary of Whiteness tests validations

Method	Model	Error energy	Maximum $RN(i)$	$RN(i)$ over limit
<i>XOLOE</i>	$n = 40$	$1.3307e-06$	$0.0154$	15
<i>XOLOE</i>	$n = 38$	$1.3337e-06$	$0.0177$	14

## 5. CONTROLLER DESIGN

The basic specifications are that the attenuation of two tonal disturbances located at 170 Hz and 285 Hz must be at least  $-40$  dB, and the maximum amplification at other frequencies be less than 7 dB. In order to strongly attenuate the two tonal disturbances the IMP has been used. This requires that the controller's fixed part  $H_s$  incorporates the disturbance's model. See (Landau et al., 2016). The tonal disturbances can be modeled by:

$$p(t) = \frac{N_p(q^{-1})}{D_p(q^{-1})} \cdot \delta(t), \quad (19)$$

with  $\delta(t)$  as a Dirac impulse.  $D_p$  has roots on the unit circle. In practice, the contribution of  $N_p$  is negligible for steady state

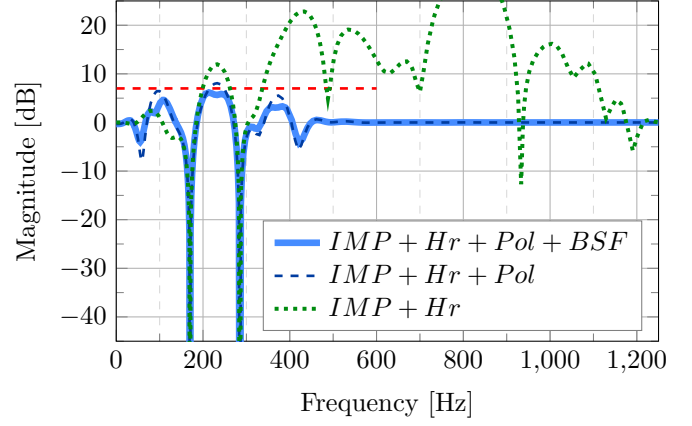


Fig. 8: Frequency characteristics for Output sensitivity,  $S_{yp}$ .

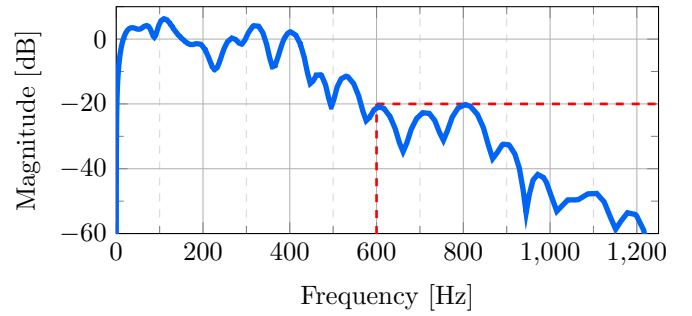


Fig. 9: Frequency characteristics for Input sensitivity,  $S_{up}$ .

analysis in comparison with  $D_p$ . So the IMP requires that the controller contains a disturbance's model, i.e.  $H_S(q^{-1}) = D_p(q^{-1})$ . For this specific case considered,  $H_S = H_{S_1}H_{S_2}$  where:

$$H_{S_i}(q^{-1}) = 1 - 2 \cos\left(2\pi \frac{f_i}{f_s}\right) q^{-1} + q^{-2}, \quad (20)$$

with  $f_1 = 170$  Hz and  $f_2 = 285$  Hz. Also, since the system has a zero gain at 0 Hz and a very low gain at 1250 Hz, the loop has been opened at these frequencies by choosing  $H_R = (1 + q^{-1})(1 - q^{-1})$ . Furthermore, in order to improve robustness, the input sensitivity function should be below  $-20$  dB at frequencies over 600 Hz (beyond the system's bandpass). The dominant closed loop poles have been chosen equal to those of the secondary path.

Fig. 8 shows the resulting output sensitivity function  $S_{yp}$  (curve  $IM + H_r$ ). The specifications for maximum gain are violated. To overcome this, 30 auxiliary real poles with value  $p_i = 0.25$  have been added in the form  $P_F(z^{-1}) = (1 - p_i z^{-1})^{n_F}$ , without augmenting the controller's order (curve  $IM + H_r + Pol$ ). The resulting sensitivity function is improved but the limit is still violated. To further shape the sensitivity function, *Band-Stop Filters* (BSF) have been used (Landau et al. (2016)); 3 on  $S_{yp}$ , and 3 on  $S_{up}$  to obtain a correct behavior (see table 2). The resulting output sensitivity function is shown in Fig. 8. Also the resulting input sensitivity function is shown in Fig. 9.

Table 2: Band-Stop Filters for sensitivity functions.

S <sub>yp</sub>		S <sub>up</sub>	
Freq.[Hz]	Ampli.[dB]	Freq.[Hz]	Ampli.[dB]
90	-6.00	600	-6.00
231	-8.00	800	-1.00
370	-5.00	945	+5.00

Fig. 10 displays the system's output for a simulation using the models estimated for the primary and secondary paths. A pair of sinusoidal signals at 170 Hz and 285 Hz were used as disturbances  $p(t)$  from 1 s to 11 s. Control starts at 6 s and ends at 11 s. A global attenuation of 86.4 dB was achieved, with attenuations of  $-88.6$  dB at 170 Hz, and  $-94$  dB at 285 Hz.

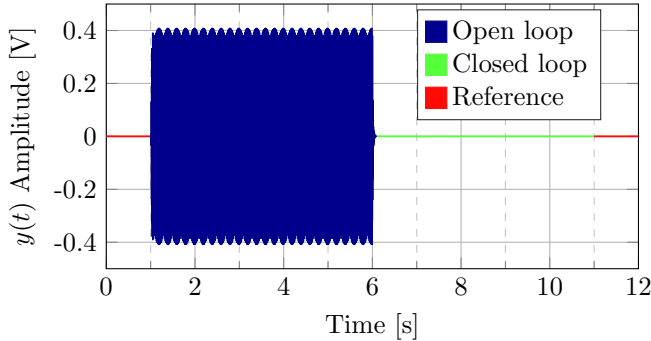


Fig. 10: Simulation results.

## 6. EXPERIMENTAL RESULTS

The experimental results have been obtained by implementing the designed controller on the test-bench described in Section 2.

Fig. 11 shows the result for a real time test. Two tonal sinusoidal signals at 170 Hz and 285 Hz were used as disturbances  $p(t)$  from 1 s to 11 s. Control starts by closing the loop at 6 s and ends at 11 s. Performances during the first second and the last one are used as a reference for the ambient noise (no control, no disturbance). A global attenuation of 76.88 dB was achieved, with disturbance attenuations of  $-94.5$  dB at 170 Hz, and  $-94$  dB at 285 Hz. These results are very close to those obtained in simulation. Fig. 12 displays the effective residual PSD estimation, calculated as a difference between the open-loop PSD and the closed-loop PSD of the residual noise.

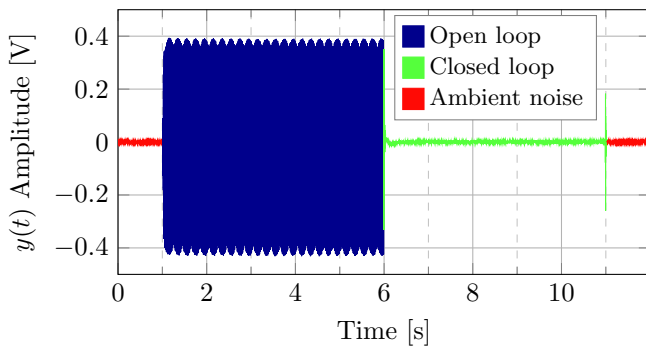


Fig. 11: Real-time experiment results: tonal disturbances.

Fig. 13 displays the results for a second real-time test. Two pairs of sinusoidal interference signals (170 Hz+170.5 Hz and 285 Hz+285.5 Hz) with amplitude of 0.14 V were used as disturbances  $p(t)$  from 1 s to 20 s. Control starts by closing the loop at 10 s and ends at 20 s. Performances during first and last second are used as a reference for ambient noise again. A global attenuation of 59.55 dB was achieved.

## REFERENCES

Ben Amara, F., Kabamba, P., and Ulsoy, A. (1999). Adaptive sinusoidal disturbance rejection in linear discrete-time sys-

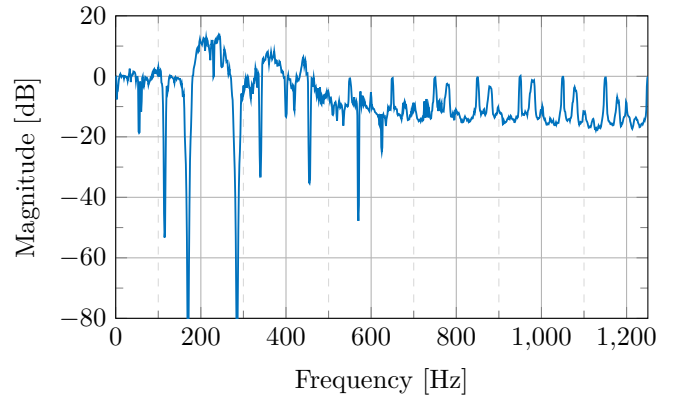


Fig. 12: Effective residual attenuation PSD estimation.

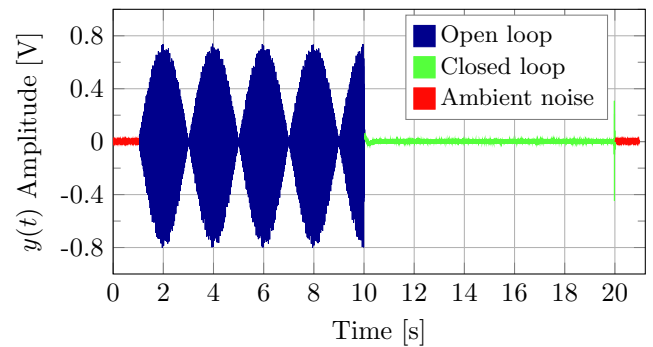


Fig. 13: Interference attenuation: residual noise in open loop and closed loop.

- tems - Part II: Experiments. *Journal of Dynamic Systems Measurement and Control*, 121, 655–659.
- Carmona, J.C. and Alvarado, V.M. (2000). Active noise control of a duct using robust control theory. *IEEE-CST*, 8(6), 930–938.
- Duong, H.N. and Landau, I.D. (1996). An IV Based Criterion for Model Order Selection. *Automatica*, 32(6), 909–914.
- Elliott, S. and Nelson, P. (1994). Active noise control. *Noise / News International*, 75–98.
- Elliott, S. and Sutton, T. (1996). Performance of feedforward and feedback systems for active control. *IEEE Speech Audio Proces.*, 4(3), 214–223.
- Kuo, S. and Morgan, D. (1999). Active noise control: a tutorial review. *Proceedings of the IEEE*, 87(6), 943 – 973.
- Landau, I.D., Airimioaie, T.B., and Castellanos-Silva, A. (2016). *Adaptive and Robust Active Vibration Control*. Springer, London.
- Ljung, L. (1999). *System Identification - Theory for the User*. Prentice Hall, Englewood Cliffs, second edition.
- Nelson, P. and Elliott, S. (1993). *Active Control of Sound*. Academic Press.
- Widrow, B. and Stearns, S. (1985). *Adaptive Signal Processing*. Prentice-Hall, Englewood Cliffs, New Jersey.
- Zeng, J. and de Callafon, R. (2006). Recursive filter estimation for feedforward noise cancellation with acoustic coupling. *Journal of Sound and Vibration*, 291(3-5), 1061 – 1079.
- Zimmer, B.J. and Lipshitz, S.P. (2003). An improved acoustic model for active noise control in a duct. *Journal of Dynamic Systems, Measurement, and Control*, 125, 382–395.